7688–7701 *Nucleic Acids Research, 2015, Vol. 43, No. 16* *Published online 5 August 2015*
doi: 10.1093/nar/gkv767

Agonistic aptamer to the insulin receptor leads to biased signaling and functional selectivity through allosteric modulation

Na-Oh Yunn[1], Ara Koh[2], Seungmin Han[2], Jong Hun Lim[3], Sehoon Park[2], Jiyoun Lee[2], Eui Kim[4], Sung Key Jang[1,2,4], Per-Olof Berggren[4,5] and Sung Ho Ryu[1,2,4,*]

[1]The School of Interdisciplinary Bioscience and Bioengineering, Pohang University of Science and Technology, Pohang 790-784, South Korea, [2]The Department of Life Sciences, Pohang University of Science and Technology, Pohang 790-784, South Korea, [3]The POSTECH Aptamer Initiative Program, POSTECH Biotech Center, Pohang University of Science and Technology, Pohang 790-784, South Korea, [4]The Division of Integrative Bioscience and Biotechnology, Pohang University of Science and Technology, Pohang 790-784, South Korea and [5]The Rolf Luft Research Center for Diabetes and Endocrinology, Karolinska Institutet, SE-171 76 Stockholm, Sweden

Received April 14, 2015; Revised July 15, 2015; Accepted July 16, 2015

ABSTRACT

Due to their high affinity and specificity, aptamers have been widely used as effective inhibitors in clinical applications. However, the ability to activate protein function through aptamer-protein interaction has not been well-elucidated. To investigate their potential as target-specific agonists, we used SELEX to generate aptamers to the insulin receptor (IR) and identified an agonistic aptamer named IR-A48 that specifically binds to IR, but not to IGF-1 receptor. Despite its capacity to stimulate IR autophosphorylation, similar to insulin, we found that IR-A48 not only binds to an allosteric site distinct from the insulin binding site, but also preferentially induces Y1150 phosphorylation in the IR kinase domain. Moreover, Y1150-biased phosphorylation induced by IR-A48 selectively activates specific signaling pathways downstream of IR. In contrast to insulin-mediated activation of IR, IR-A48 binding has little effect on the MAPK pathway and proliferation of cancer cells. Instead, AKT S473 phosphorylation is highly stimulated by IR-A48, resulting in increased glucose uptake both *in vitro* and *in vivo*. Here, we present IR-A48 as a biased agonist able to selectively induce the metabolic activity of IR through allosteric binding. Furthermore, our study also suggests that aptamers can be a promising tool for developing artificial biased agonists to targeted receptors.

INTRODUCTION

Aptamers are single-strand oligonucleotides artificially isolated by an *in vitro* selection process called Systematic Evolution of Ligands by EXponential Enrichment (SELEX) (1,2). Due to their unique three-dimensional structure, aptamers can strongly interact with specific regions of target molecules. Based on this property, aptamers are widely used in many applications as target-specific binders with high affinity and specificity.

Most efforts to develop functional aptamers focused on their inhibitory effects on target molecules. In clinical applications, a variety of inhibitory aptamers have been developed to treat diseases by effectively disrupting the action of target molecules (e.g. Macugen, an anti-VEGF aptamer and AS1411, an anti-nucleolin aptamer) (3–5). However, given that molecular interaction is necessarily followed by conformational change, it is reasonable to assume that aptamer–protein interaction can also activate the function of protein if it induces the proper conformational change. Thus, in theory, aptamers have the potential to act as functional agonists by mimicking specific protein–protein interactions. However, the development of agonistic aptamers that directly activate target functions remains a challenging task at present.

For the proof of concept that the development of agonistic aptamers is possible, we generated aptamers against membrane receptors and screened them by analyzing receptor activation. Membrane receptors are ideal targets for the development of agonistic aptamers. First, aptamers against the extracellular domains of membrane receptors do not need to be capable of membrane penetration. Generally, negatively charged oligonucleotides such as aptamers cannot penetrate plasma membranes without delivery systems

*To whom correspondence should be addressed. Tel: +82 54 279 2292; Fax: +82 54 279 0645; Email: sungho@postech.ac.kr

(6). Second, the development of receptor modulators is a valuable tool for drug discovery because membrane proteins account for ∼60% of all approved drug targets (7,8).

In this study, we chose the insulin receptor (IR) as the target receptor for the development of an aptamer agonist. The IR consists of two extracellular α-subunits that contain insulin binding sites and two transmembrane β-subunits with kinase activity. Insulin binding to the IR results in autophosphorylation of intracellular tyrosine residues, which increases IR kinase activity and initiates a cascade of intracellular signaling events (9). IR signaling mediates a wide range of metabolic and mitogenic functions and, importantly, plays a critical role in the homeostasis of blood glucose by regulating glucose transporter 4 (GLUT4) translocation to the cell surface in adipose tissue and muscle (10). Diabetes mellitus develops when GLUT4 translocation is impaired by insulin resistance or insufficient insulin (11). Accordingly, the development of agonists able to effectively stimulate IR activity is considered an important goal for diabetes care.

Here, we present an agonistic IR aptamer, IR-A48, which binds to an allosteric site of the IR that is distinct from the insulin binding site. Interestingly, we found that IR-A48 not only preferentially stimulates Y1150 phosphorylation in the IR kinase domain, but also has biased activity toward the IRS-AKT S473 pathway, stimulating glucose uptake rather than activation of the MAPK pathway and subsequent cell proliferation. Our findings suggest that IR-A48 is a biased agonist able to specifically regulate the insulin signaling pathway (i.e. metabolic over mitogenic activity). These findings comprise a pilot study that provides the rationale for the development of allosteric aptamer agonists able to selectively regulate the functions of various receptors.

MATERIALS AND METHODS

Reagents and antibodies

Aptamers were synthesized from Aptamer Science, Inc. (Pohang, Korea) or ST Pharm (Siheung, Korea). Bovine insulin, FITC-labeled insulin, LY-294002, dexamethasone and 3-isobutyl-1-methylxanthine (IBMX) were purchased from Sigma-Aldrich (St Louis, MO, USA). Phospho-peptides for ELISA assay were synthesized by Selleckchem (Houston, TX, USA). Anti-IR β-subunit (C-19), anti-IGF-1R β-subunit (C-20), anti-phospho-IR (10C3, Y1150/Y1151), anti-phospho-IRS1 (Y632) and anti-phospho-Shc (Y239/Y240) antibodies were purchased from Santa Cruz Biotechnology (Santa Cruz, CA, USA). Anti-phospho-tyrosine (4G10), anti-phospho-IRS1 (Y612) human/(Y608) mouse and anti-phospho-IR (Y1146) antibodies were purchased from Millipore (Darmstadt, Germany). Anti-phospho-IR (Y960), anti-phospho-IR (pAb, Y1150/Y1151), anti-phospho-IR (Y1316), anti-phospho-IR (Y1322), anti-phospho-IR (Y1146/Y1150/Y1151), alkaline phosphatase (AP)-labeled anti-rabbit/mouse antibodies and Disodium 3-(5'-chloro-4-methoxyspiro[1,2-dioxetane-3,2'-tricyclo[3.3.1.13,7]decan]-4-yl)phenyl phosphate (CSPD) substrate for AP were purchased from Invitrogen (Carlsbad, CA, USA). Anti-phospho-AKT (S473), anti-phospho-AKT (T308), anti-phospho-ERK1/2 (T202/Y204), anti-phospho-FoxO1/3a (T24/T32) and anti-phospho-AS160 (T642) antibodies were purchased from Cell Signaling Technology (Danvers, MA, USA). IRdye 800-conjugated anti-rabbit/mouse antibodies were purchased from Rockland (Limerick, PA, USA) and HRP-conjugated anti-rabbit/mouse antibodies were purchased from KPL (Gaithersburg, MD, USA).

In vitro selection of IR aptamers

To identify IR-specific aptamers, we performed a SELEX process as previously described (12). Briefly, a modified single-stranded DNA (ssDNA) library with a 40mer random region (N_{40}) containing 5-[N-(1-naphthylmethyl)carboxamide]-2′-deoxyuridine (Nap-dU) in place of dT was prepared. The random regions were flanked by 20mer constant regions for polymerase chain reaction (PCR) with the following sequence: 5′-TATGAGTGACCGTCCGCCTG-N_{40}-CAGCCACACCACCAGCCAAA-3′. The ssDNA library was incubated with his-tagged recombinant IR extracellular domain (His 28-Lys 944) (R&S Systems, MN, USA) in selection buffer [40 mM HEPES (pH 7.5), 102 mM NaCl, 5 mM KCl, 5 mM $MgCl_2$ and 0.05% Tween-20]. After ssDNA binding, IR proteins were partitioned by immobilizing them on Dynabeads TALON (Invitrogen, Carlsbad, CA, USA) and unbound ssDNAs were removed by washing with selection buffer. ssDNAs were extracted and amplified by conventional PCR using a 5′-OH terminal biotinylated reverse primer. After eight rounds of SELEX, the enriched ssDNA pool was cloned and sequenced.

Aptamer binding assay

The binding affinity of the aptamer to the extracellular domains of IR (His 28-Lys 944) and IGF-1R (Gln 31Asn 932) was analyzed by filter binding assay. First, the 5′-end of the aptamer was labeled with [α-32P] adenosine triphosphate. After heating at 95°C for 3 min and then slow cooling to 37°C at 0.1°C/s in binding buffer [40 mM HEPES (pH 7.5), 120 mM NaCl, 5 mM KCl, 5 mM $MgCl_2$ and 0.002% Tween-20] to reconstitute the aptamer structure, the aptamer was incubated with purified recombinant IR or IGF-1R at various concentrations for 30 min at 37°C. To pull down the aptamer–protein complexes, the solution was incubated with Zorbax silica beads (Agilent, CA, USA) for 1 min with shaking. The aptamer–protein complex bound to the beads was partitioned through nitrocellulose filter plates (Millipore, MA, USA) and washed in binding buffer to remove unbound aptamer. The amount of radiolabeled aptamer that interacted with proteins was detected by exposure to photographic film and quantified using a Fuji FLA-5000 Image Analyzer (Tokyo, Japan). The dissociation constant (K_d) of the aptamers was determined by fitting the binding data to a one-site saturation equation using the SigmaPlot program.

Cell culture and adipocyte differentiation

HEK293 and 3T3-L1 cells were purchased from ATCC (Manassas, VA, USA), and MCF-7 cells were purchased

from KCLB (Korea Cell Line Bank, Seoul), and Rat-1 cells overexpressing human IR were kindly provided by Dr Nicholas J. G. Webster from the University of California, San Diego. HEK293, Rat-1/hIR and MCF-7 cells were maintained in high glucose Dulbecco's modified Eagle's medium (DMEM) with 10% (vol/vol) fetal bovine serum (FBS, Lonza) and 3T3-L1 pre-adipocytes were maintained in high glucose DMEM with 10% bovine serum (BS, Gibco) at 37°C under a humidified atmosphere containing 5% CO_2. For adipocyte differentiation, 3T3-L1 pre-adipocytes were cultured for 2 days past confluence. Differentiation was initiated by changing the medium to DMEM containing 1 μM dexamethasone, 500 nM IBMX, 850 nM insulin and 10% FBS. After 2 days, the medium was replaced with DMEM containing 850 nM insulin and 10% FBS and then incubated for two additional days. Finally, the medium was changed to DMEM containing only 10% FBS and incubated for 4–5 days until at least 90% of the cell population exhibited accumulation of lipid droplets.

Cell experiments

Before insulin or aptamer stimulation, the cells were incubated in DMEM without FBS for 3 h and then incubated in Krebs-Ringer HEPES buffer [25 mM HEPES (pH 7.4), 120 mM NaCl, 5 mM KCl, 1.2 mM $MgSO_4$, 1.3 mM $CaCl_2$ and 1.3 mM KH_2PO_4] for 1 h. For the cell experiments, the aptamers and insulin were prepared in Krebs-Ringer HEPES buffer. All aptamer samples were heated for 5 min at 95°C and slowly cooled to room temperature to reconstitute the tertiary structure of the aptamer.

Western blot and immunoprecipitation

To prepare total cell lysate, harvested cells were lysed in lysis buffer [50 mM Tris–HCl (pH 7.4), 150 mM NaCl, 1 mM ethylenediaminetetraacetic acid (EDTA), 20 mM NaF, 10 mM β-glycerophosphate, 2 mM Na_3VO_4, 1 mM PMSF, 10% glycerol, 1% Triton-X and protease inhibitor cocktails]. Soluble cell lysate was isolated by centrifugation at 14 000 rpm for 15 min at 4°C. For immunoprecipitation, the isolated cell lysate was incubated with 2 μg of antibodies overnight at 4°C and Protein A agarose beads were added to pull down the antibodies. After sodium dodecyl sulphate-polyacrylamide gel electrophoresis, the proteins were transferred to membranes and incubated in primary antibodies overnight at 4°C. Blotting was performed using a LI-COR Odyssey infrared imaging system or enhanced chemiluminescence (Thermo Scientific, MA, USA).

Insulin competition assay

Rat-1/hIR cells were grown in 100 mm dishes to 70% confluence. After cell detachment using phosphate buffered saline (PBS) containing 5 mM EDTA, the cells were incubated with blocking buffer (PBS, 1% BSA and 0.1% NaN_3) for 30 min at 4°C. Next, the cells were divided into equal aliquots and 50 nM FITC-labeled insulin was added with IR-A48 or native insulin. The cells were incubated for 1 h at 4°C to allow the binding reaction to reach equilibrium, and the cells were washed twice with cold PBS. After fixation with PBS containing 4% paraformaldehyde for 30 min at room temperature (RT), IR-bound FITC-labeled insulin was measured by flow cytometry (BD FACSCanto^{TM} II).

ELISA

Synthetic phospho-peptides at 20 pmol/100 μl (MTRDIYETD-pY-pY-RKGGKGLL, MTRDIYETD-pY-YRKGGKGLL and MTRDIYETDY-pY-RKGGKGLL) were covalently cross-linked to 96-well plates (Corning, MA, USA) coated with N-oxysuccinimide ester groups in PBS overnight at 4°C. After blocking with PBS containing 1% BSA for 1 h at RT, the plates were washed once with Tris-Tween Buffered Saline (TTBS) buffer [50 mM Tris–HCl (pH 7.6), 150 mM NaCl and 0.05% Tween-20] and incubated with primary antibodies diluted 1:1000 in TTBS for 1 h at RT. The plates were then washed three times in TTBS and incubated with AP-conjugated secondary antibodies diluted 1:2000 for 1 h at RT and then washed three times with TTBS. CSPD substrate for AP was added at 100 μl per well and the chemiluminescence was measured using a luminometer (Luminoskan Ascent).

2-Deoxy-D-glucose uptake

The fully differentiated 3T3-L1 adipocytes were serum-starved for 3 h in DMEM without FBS and glucose-starved for 1 h in Krebs-Ringer HEPES buffer prior to insulin or aptamer stimulation. After insulin or aptamer stimulation for the indicated times, the cells were incubated with 2-deoxy[14C]glucose (0.1 μCi/ml) for 10 min and washed three times in cold PBS containing 25 mM D-glucose. The cells were lysed in 0.5 N NaOH and 1% sodium dodecyl sulphate solution and glucose uptake was measured by liquid scintillation counter.

Cell proliferation assay

MCF-7 cells were plated at 10^4 cells/well in 24-well plates in DMEM containing 10% FBS [low glucose (1 g/l) without phenol red or pyruvate]. After 24 h, the cells were serum-starved in DMEM containing 0.5% FBS for an additional 24 h. Next, insulin and aptamers were added and replaced every 24 h for a total of 72 h. The cells were fixed with 4% paraformaldehyde in PBS for 30 min and stained with 1 μM SYTO 60 in PBS for 1 h. The cell numbers were analyzed by measuring the fluorescence of SYTO 60-stained DNA using a LI-COR Odyssey infrared imaging system.

Glucose lowering effect in mice

All animal experiments were approved by the POTECH Animal Use and Care Committee. C57Bl/6J male mice (8 weeks old) were maintained on a 12 h light/dark cycle with regular unrestricted diets. Before insulin or aptamer injection, the mice were starved for 12 h. Insulin and aptamers were dissolved in PBS and administrated to the mice intravenously. Blood was collected from the tail vein at 15, 30, 60, 90 and 120 min after injection, and blood glucose levels were measured using a glucometer (Accu-Check Active; Roche Diagnostics).

RESULTS

Identification of an agonistic aptamer for the insulin receptor

Based upon the concept that modulating the conformation of the extracellular domain of IR can be translated to the activation of intracellular functions, we used SELEX to develop IR aptamers capable of binding to the extracellular domain of human IR. SELEX was performed using single-strand DNA libraries that consist of a 40mer random region and both sides of 20mer constant regions and purified recombinant IR protein that consists of the extracellular domain (His 28-Lys 944) with a C-terminal His tag. Thymines in the random regions were replaced with 5-[N-(1-naphthylmethyl)carboxamide]-2′-deoxyuridine (Nap-dU) to enhance the affinity and specificity of protein–aptamer interactions (13).

To identify agonistic IR aptamers, we analyzed whether or not the aptamers (1 μmol/l) increased V-akt murine thymoma viral oncogene homolog (AKT) S473 phosphorylation in HEK293 cells over-expressing human IR. Although most aptamers had no effect on insulin signaling, one IR aptamer, IR-A48F, significantly stimulated AKT phosphorylation (data not shown). The sequence of IR-A48F consists of 80 nt and contains 8 Nap-dUs in the random region (Figure 1A). To determine the minimal binding domain, we performed aptamer truncation based on the secondary structure of IR-A48F. The secondary structure predicted by the Mfold program showed that 33 internal nucleotides containing 6 Nap-dUs form a stable stem-loop structure (Figure 1B). The results of binding assay showed that the internal stem-loop sequence (IR-A48) binds to IR with similar affinity (3.5 nM K_d) as IR-A48F (6.9 nM K_d) (Figure 1C). Moreover, IR-A48 appears to be highly specific to IR, because no significant binding was detected toward insulin-like growth factor 1 receptor (IGF-1R), which is structurally similar to IR (14). Thus, these results indicate that the binding of IR-A48 is highly specific to IR, in contrast to insulin, which binds both IR and IGF-1R. Thus, all subsequent experiments were performed using IR-A48.

IR-A48 binds to an allosteric site of IR

To investigate the binding properties of IR-A48, we performed an insulin competition assay, followed by flow cytometry. Rat-1 cells over-expressing human IR (Rat-1/hIR) were incubated with FITC-labeled insulin (50 nmol/l) and various concentrations of IR-A48 (0.04, 0.16, 0.63, 2.5 and 10 μmol/l) and FITC fluorescence was measured to assess changes in insulin binding. Despite its agonistic effect, IR-A48 did not interfere with the binding of insulin to IR, even at concentrations 200-fold higher than that of insulin (Figure 2A). This indicates that IR-A48 is an allosteric aptamer that binds to a site distinct from the orthosteric insulin binding site.

Consistent with the allosteric binding of IR-A48, insulin-induced downstream signaling (phosphorylation of Insulin receptor substrate (IRS), AKT and Extracellular signal-regulated kinases (ERK)) was not affected by IR-A48 treatment in Rat-1/hIR cells (Figure 2B). However, the IR autophosphorylation patterns induced by IR-A48 are different from those produced by insulin. While both insulin and IR-A48 induced Y1150/Y1151 phosphorylation in the IR kinase domain that was cooperatively increased when added in combination, total tyrosine phosphorylation of IR was increased dramatically by insulin stimulation, but increased only slightly by IR-A48 stimulation. In addition, phosphorylation of IRS Y608 and AKT S473 was increased by IR-A48, but no changes in the phosphorylation of ERK T202/Y204 and AKT T308 were detected (Figure 2B). Taken together, these results show that the allosteric binding of IR-A48 induces IR autophosphorylation, but the activity seems to be biased toward specific tyrosine residues in the IR kinase domain.

IR-A48 preferentially stimulates IR Y1150 phosphorylation

Insulin binding to IR results in autophosphorylation of seven tyrosine residues in the intracellular β-subunits (Y953 and Y960 in the juxtamembrane region; Y1146, Y1150 and Y1151 in the kinase domain; and Y1316 and Y1322 in the carboxy-terminus) (9). Therefore, we investigated the effect of IR-A48 on the tyrosine phosphorylation of specific IR residues using six commercially available antibodies (for all residues except IR pY953, for which an antibody is not yet available). While insulin robustly increased the phosphorylation of Y960, Y1146, Y1150, Y1151, Y1316 and Y1322 of IR, IR-A48 induced increased phosphorylation of only the Y1150/Y1151 residues in the IR kinase domain (Figure 3A). Despite the significant difference with insulin, Y1150/Y1151 phosphorylation by IR-A48 was not an off-target effect of Nap-dU containing oligonucleotides or modified bases (Nap-dU). A scrambled aptamer (IR-A48 RC, reverse complementary sequence of IR-A48), a random Nap-dU DNA library used for SELEX and Nap-dU mononucleotide had no effect on Y1150/Y1151 phosphorylation of IR (Supplementary Figure S1). To clearly confirm the Y1150/Y1151-biased phosphorylation by IR-A48, we used two different commercial antibodies to detect Y1150/Y1151 phosphorylation: 10C3 (sc-81500) from Santa Cruz and pAb (44804G) from Invitrogen. However, in contrast to 10C3, which was previously used to detect Y1150/Y1151 phosphorylation, the polyclonal antibody (pAb) did not detect any phosphorylation by IR-A48 (Figure 3A).

Because Y1150 and Y1151 are independently phosphorylated during IR autophosphorylation, we hypothesized that the two phospho-antibodies have different binding affinities for mono-pY1150, mono-pY1151 and dual-pY1150/pY1151 (15). To clarify this issue, we determined the binding specificity of these two antibodies by performing an ELISA using synthetic phospho-peptides corresponding to pY1150, pY1151 or pY1150/pY1151. Although the two antibodies are described as able to detect dual pY1150/pY1151 (as per the provided manuals from the manufacturer), they have significantly different binding specificities for the mono-pY1150 peptide. The 10C3 antibody detected phosphorylation of both the dual-pY1150/pY1151 and mono-pY1150 peptides to a similar degree, but the polyclonal antibody (pAb) bound strongly to only the dual pY1150/pY1151 peptide (Figure 3B). Taken together, these data demonstrate that IR-A48 is a bi-

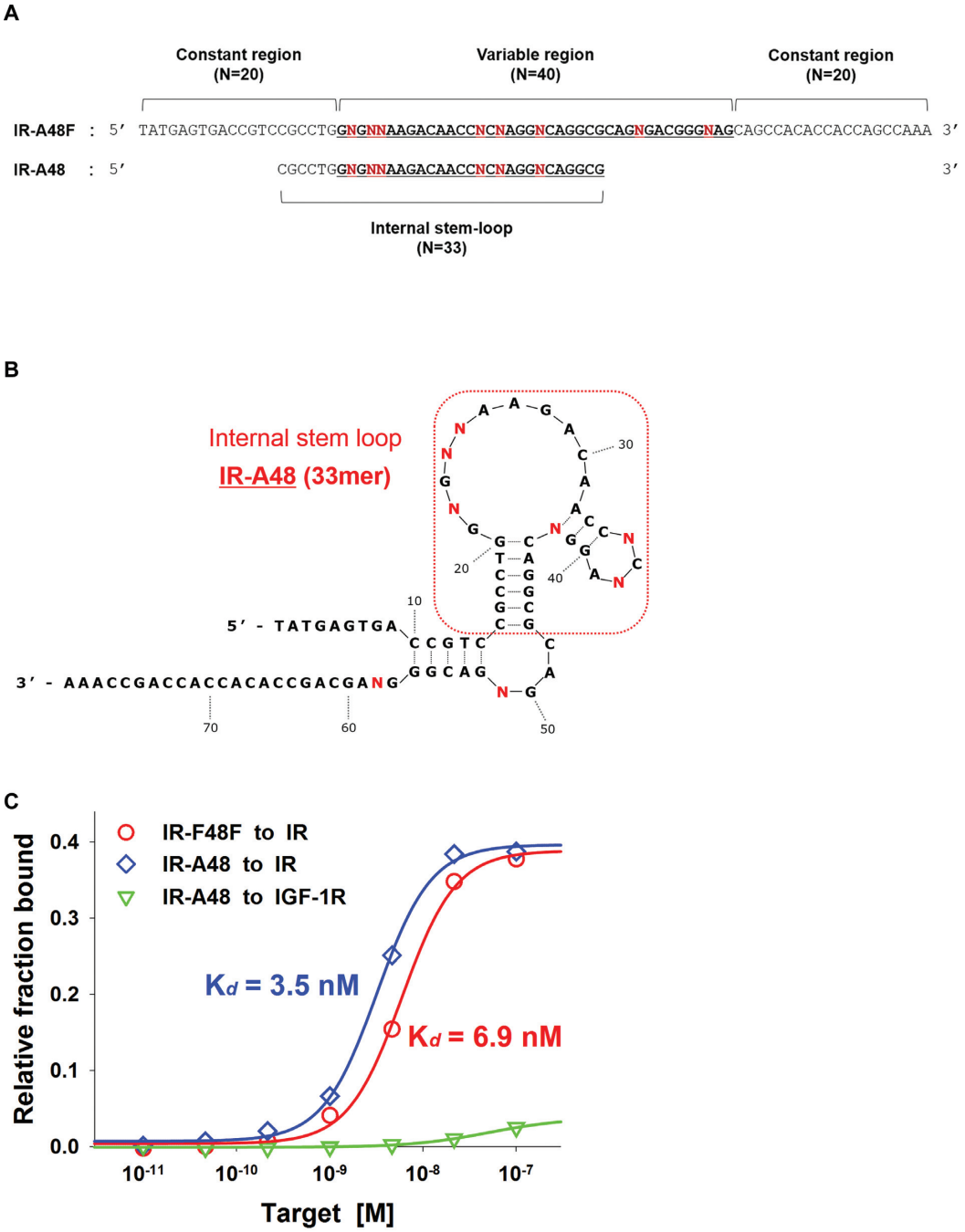

Figure 1. Properties and truncation of IR-A48. (**A**) Comparison of the full (IR-A48F) and truncated (IR-A48) sequences of the identified agonistic IR aptamer. 'N' indicates Nap-dU. (**B**) The secondary structure of IR-A48F was obtained from Mfold software. The dot box highlights the internal 33 nt (IR-A48) that form the stem-loop structure. (**C**) Dose-dependent binding to IR and IGF-1R was measured to compare affinity between IR-A48F and IR-A48. The dissociation constant (K_d) was determined by fitting the data to a one-site saturation model.

ased IR agonist that preferentially induces Y1150 phosphorylation in the IR kinase domain.

Even with the high structural similarity between IR and IGF-1R, IR-A48 did not bind to IGF-1R (Figure 1C). To confirm this, we used the 10C3 antibody to assess the effect of IR-A48 on phosphorylation of IGF-1R Y1135, which is homologous to Y1150 of IR. As expected, unlike insulin or IGF-1, IR-A48 did not increase phosphorylation of IGF-1R Y1135 in HeLa cells (Figure 3C).

IR-A48 differently modulates downstream signaling in 3T3-L1 adipocytes

Next, we decided to confirm whether Y1150-biased phosphorylation by IR-A48 differently modulates downstream signaling compared to insulin. The phosphorylation of tyrosine residues on IR β-subunits plays two roles in the insulin signaling process. First, phosphorylations in the kinase domain (Y1146, Y1150 and Y1151) regulate IR kinase

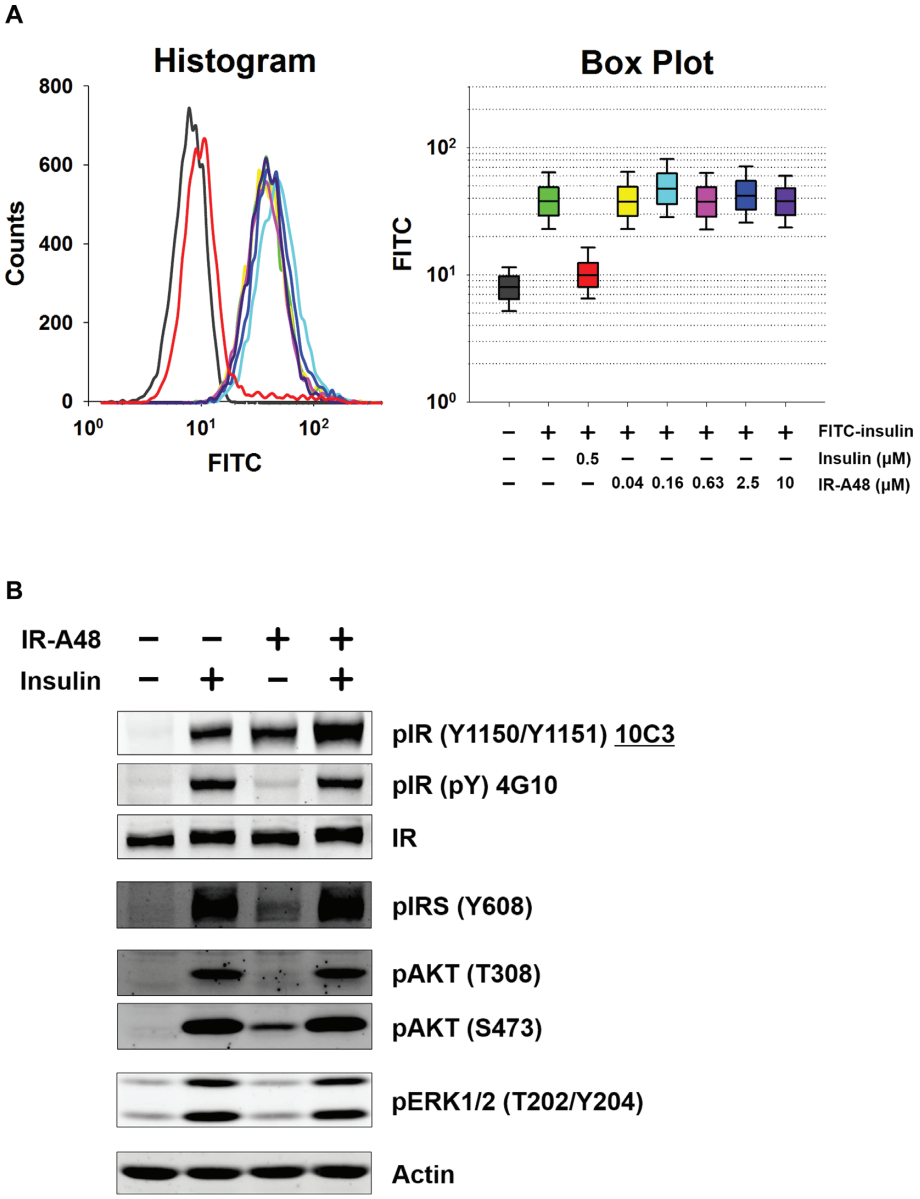

Figure 2. Allosteric binding of IR-A48 and insulin receptor autophosphorylation. (**A**) Insulin competition assay was used to confirm the allosteric binding of IR-A48 using flow cytometry. The box plot displays the statistical distribution of FITC fluorescence from the results of the histogram. The horizontal line in the box indicates the median value. The vertical box indicates the 25th or 75th percentile, and the vertical line indicates the maximum or minimum value excluding outliers. (**B**) The effect of IR-A48 on insulin activity in Rat-1/hIR cells. Cells were stimulated with 50 nmol/l insulin or/and 200 nmol/l IR-A48 for 10 min and phosphorylation was detected by western blotting.

activity (16). Second, phosphorylated tyrosines in the juxtamembrane (Y960) and C-terminal regions (Y1322) function as binding sites for adaptor proteins (17–20). Thus, considering the Y1150-biased phosphorylation, IR-A48 would not be expected to be able to fully activate downstream signaling due to the low levels of phosphorylation of other tyrosine residues.

However, unexpectedly, IR-A48 significantly activated signaling in a manner comparable to insulin. In fully differentiated 3T3-L1 adipocytes stimulated by insulin (50 nmol/l), the phosphorylation of IR and major insulin signaling proteins such as IRS, AKT and ERK reached a maximal response in <5 min and gradually disappeared over several minutes to hours (Figure 4A). In contrast to insulin, IR-A48 (200 nmol/l) slowly increased the phosphorylation of IR (Y1150), IRS (Y608, Y632), AKT (T308, S473), AS160 (T642), GSK3 α/β (S21/S9) and FOXO1/3a (T24/T32) by 2 h and sustained the phosphorylation for over 4 h. IR Y960 was still not significantly phosphorylated by IR-A48 relative to insulin even after prolonged stimulation of up to 8 h. The slow signaling kinetics of IR-A48 was not restricted to 3T3-L1 adipocytes, as we observed the Y1150-biased IR phosphorylation by IR-A48 slowly increased for 2 h and reached a plateau that was maintained despite prolonged stimulation for over 8 h in Rat-1/hIR cells (Supplementary Figure S2). Moreover, Nap-dU

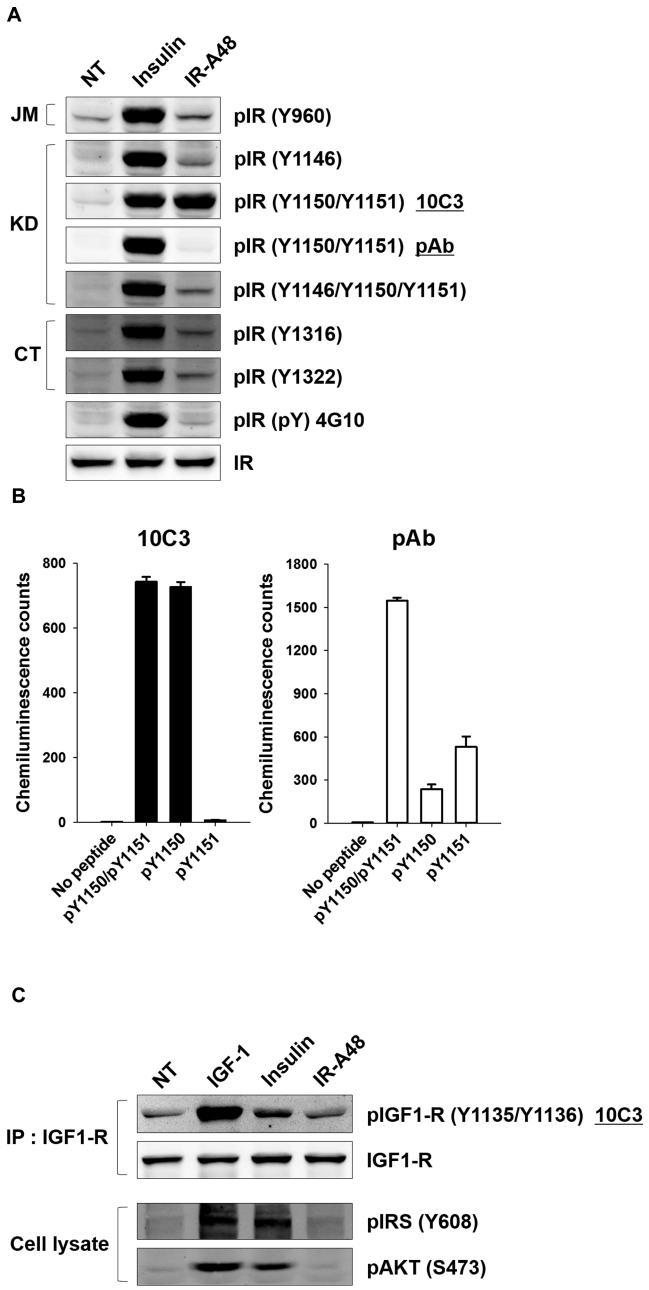

Figure 3. Y1150-biased phosphorylation in the IR kinase domain by IR-A48. (**A**) The phosphorylation of six tyrosine residues of IR was analyzed using specific phospho-antibodies. Rat-1/hIR cells were stimulated with 200 nmol/l IR-A48 and 50 nmol/l insulin for 10 min. (**B**) Specificity of the phospho-antibodies 10C3 and pAb for mono-pY1150, mono-pY1151 and dual-pY1150/pY1151 peptides. 10C3 is a monoclonal antibody purchased from Santa Cruz (sc-81500) and pAb is a polyclonal antibody purchased from Invitrogen (44804G). Data represent the mean ± S.E. of four biological replicates and similar results were obtained from two independent experiments. Black bar, 10C3; white bar, pAb. (**C**) Non-cross-reactivity of IR-A48 with IGF-1R. Following incubation of HeLa cells with 50 nmol/l IGF-1, 100 nmol/l insulin and 1 μmol/l IR-A48 for 1 h, IGF-1R was immunoprecipitated. The monoclonal antibody 10C3 was used to detect pY1135 of IGF-1R.

containing oligonucleotides and Nap-dU mononucleotide also did not stimulate downstream signaling in 3T3-L1 adipocytes (Supplementary Figure S3).

Importantly, IR-A48 showed biased activity toward subsets of the insulin signaling pathway. The level of AKT phosphorylation induced by IR-A48 was biased toward S473. IR-A48-induced AKT S473 phosphorylation reached 98% of the level of phosphorylation induced by insulin, but AKT T308 phosphorylation stayed at just 37% of the level induced by insulin (Figure 4A–C). In addition, ERK was only slightly activated by IR-A48 (Figure 4A and D). These results indicate that IR-A48 can activate signaling downstream of IR, but that the signaling cascades activated by IR-A48 are markedly different from those activated by insulin.

IR-A48 does not induce proliferation of MCF-7 cancer cells

The MAPK pathway is one of the major signaling routes induced by IR autophosphorylation and is responsible for cell proliferation (21,22). Of particular importance is the effect of insulin on cell proliferation in some cancer cell lines (23,24). Because IR-A48 did not activate the MAPK pathway (Figure 4A and D), we investigated whether IR-A48 has an effect on cell proliferation.

To analyze the mitogenic potency of IR-A48, we performed growth assays in the MCF-7 human breast cancer cell line, which is widely used to study the proliferative effect of insulin. In MCF-7 cells, insulin increased cell proliferation by up to 2.1-fold, but IR-A48 had no effect on cell proliferation (Figure 5A). Moreover, IR-A48 (1 μmol/l) did not cooperatively potentiate insulin-induced cell proliferation, even when the cells were co-incubated with increasing concentrations of insulin (Figure 5B). To rule out the possibility that IR-A48 does not activate IR in MCF-7 cells, we assessed the activation of IR and subsequent downstream signaling in MCF-7 cells. Consistent with the results in 3T3-L1 adipocytes, IR-A48 preferentially induced phosphorylation of IR Y1150 and AKT S473, but had no effect on IGF1-R, AKT T308 and ERK (Figure 5C). These data demonstrate that the signaling pathway induced by IR-A48 is completely segregated from the mitogenic insulin-IR axis.

IR-A48 stimulates glucose uptake in 3T3-L1

The metabolic function of IR is mainly regulated by the IRS-AKT pathway (25). Glucose uptake is the most important metabolic function of insulin. Insulin-induced IR autophosphorylation increases glucose uptake by inducing GLUT4 exocytosis in adipose tissue and muscle. Many studies confirmed that AKT functions as a central hub for glucose uptake by acting as a mediator between insulin signaling and regulators of GLUT4 translocation (10). Because IR-A48 stimulated AKT S473 phosphorylation in 3T3-L1 adipocytes (Figure 4A and B), we examined whether IR-A48 stimulates glucose uptake.

To investigate the effect of IR-A48-induced signaling on glucose uptake, we measured 2-deoxy-glucose uptake in 3T3-L1 adipocytes after time-dependent stimulation. Despite IR Y1150-biased phosphorylation, IR-A48 (200 nmol/l) increased glucose uptake to the same extent as insulin (50 nmol/l). In addition, consistent with its allosteric

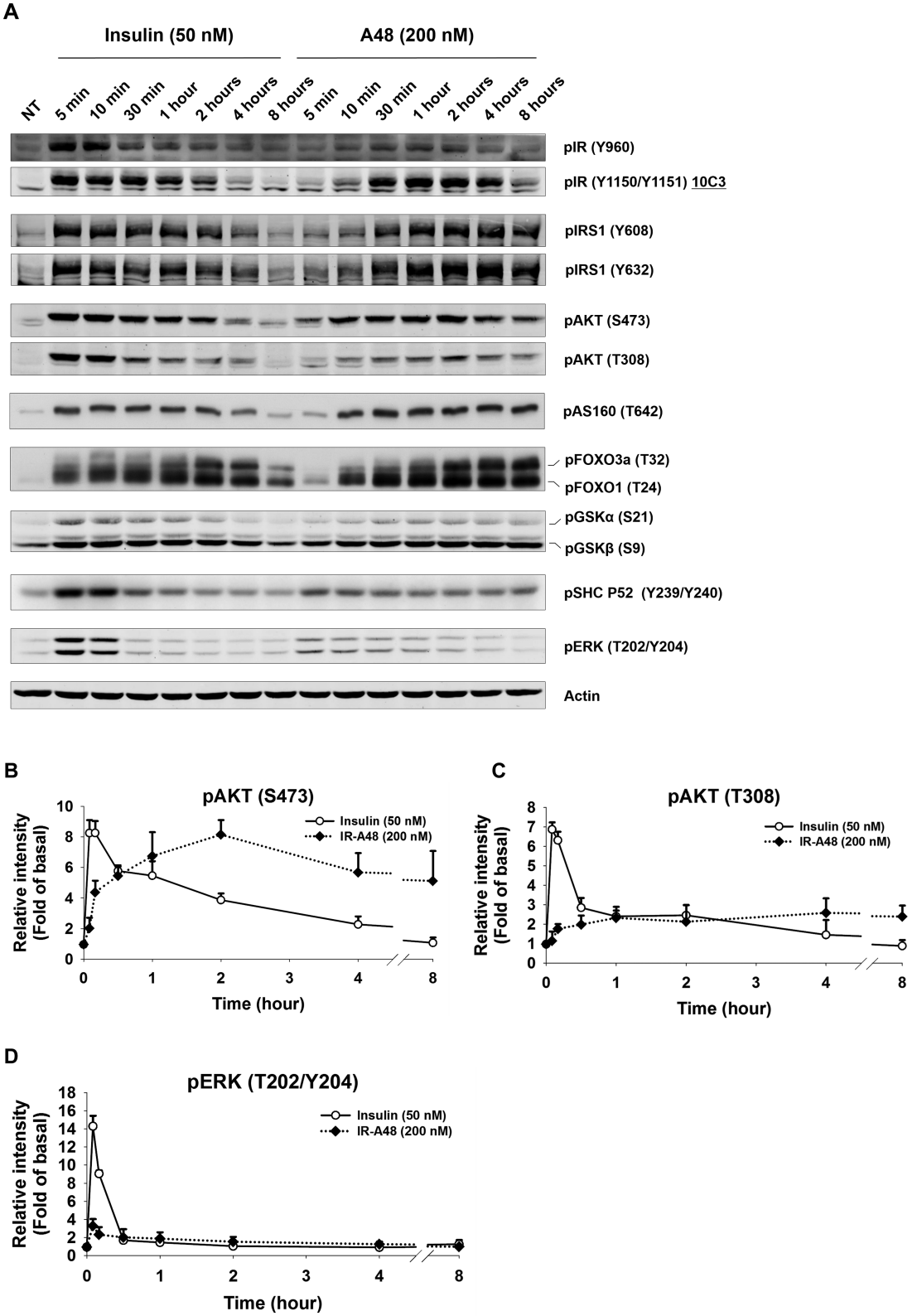

Figure 4. IR-A48 stimulated IR signaling produces distinct kinetic and phosphorylation patterns. (**A**) Fully differentiated 3T3-L1 adipocytes were stimulated with 50 nmol/l insulin and 200 nmol/l IR-A48 for the indicated times. The phosphorylation of major insulin signaling proteins was measured by western blotting. pAS160, pFOXO1/3a and pSHC were detected using ECL; the rest of the proteins were detected by an Odyssey infrared imaging system (LI-COR). The kinetics of (**B**) pAKT S437, (**C**) pAKT T308 and (**D**) pERK T202/Y204 are presented as the mean ± S.E. of three independent experiments and data were normalized to band intensity of each negative control (NT) to determine fold of basal.

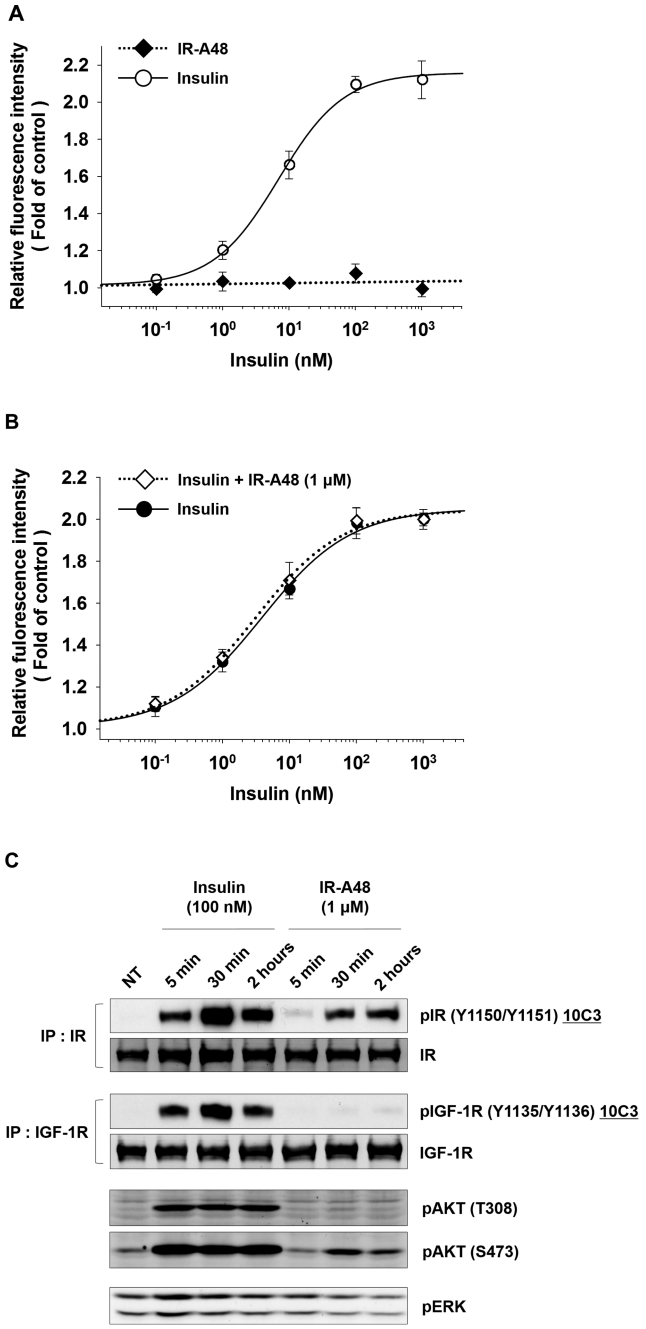

Figure 5. Proliferation of MCF-7 cells was not stimulated by IR-A48. (**A**) The effect of IR-A48 on cell proliferation was compared to that of insulin. MCF-7 cells were incubated with increasing concentrations of IR-A48 or insulin for 72 h. (**B**) To investigate whether IR-A48 can potentiate insulin-induced proliferation, cells were incubated with 1 µmol/l IR-A48 and increasing concentrations of insulin for 72 h. A proliferation assay was performed by measuring the amount of SYTO60-stained DNA using an Odyssey infrared imaging system (LI-COR) and the data were fitted to a four-parameter logistic equation. Data are presented as the mean ± S.E. of four biological replicates and similar results were obtained from three independent experiments. (**C**) The effect of IR-A48 in MCF-7 cells. MCF-7 cells were treated with 100 nmol/l insulin and 1 µmol/l IR-A48 for 5 min, 1 and 2 h.

binding to IR (Figure 2A), insulin and IR-A48 cooperatively increased glucose uptake when added in combination (Figure 6A). Similar to the phosphorylation status of IR Y1150 and AKT S473 (Figure 4A), the kinetic of glucose uptake by IR-A48 was also quite different from that of insulin. After insulin stimulation, glucose uptake reached maximal response at 30 min to 1 h and was sustained for up to 2 h before slowly decreasing to a level less than half the maximum after 8 h. However, the glucose uptake by IR-A48 slowly increased over 4 h and was sustained over 8 h (Figure 6A). IR-A48 also increased glucose uptake in L6 rat myoblast overexpressing GLUT4, which indicates that IR-A48 has cross activity to human, mouse and rat IR (Supplementary Figure S4). However, Nap-dU containing oligonucleotides and Nap-dU mononucleotide did not induce glucose uptake in 3T3-L1 adipocytes despite prolonged stimulation for 4 h (Supplementary Figure S5).

In spite of the slower kinetics, IR-A48 fully induced glucose uptake at high concentrations. We measured glucose uptake induced by insulin and IR-A48 in a dose-dependent manner based on the time points that showed maximal response (30 min for insulin and 4 h for A48). At maximal concentrations, both IR-A48 and insulin showed similar saturated levels of glucose uptake (4.2- and 4-fold, respectively; Figure 6B). However, IR-A48 exponentially increased glucose uptake in the range of 20–200 nmol/l (Hill coefficient: 2.37) in contrast to insulin, which produced a gradual dose-response curve (Hill coefficient: 0.77). Consequently, the EC_{50} value for IR-A48 was higher (66.2 nmol/l) than that for insulin (8.9 nmol/l), although the EC_{95} value for IR-A48 (202.4 nmol/l) was slightly lower than that for insulin (261.9 nmol/l). Similar to the glucose uptake patterns, the dose-dependent phosphorylation of AKT S473 and IRS Y608 by IR-A48 also showed an exponential curve (Supplementary Figure S6). It is still unclear why IR-A48 produces an exponential dose-response curve compared to insulin, but these data clearly indicate that IR-A48 can fully stimulate glucose uptake.

Phosphoinositide 3-kinase dependency of IR-A48 on glucose uptake

In insulin signaling cascades, phosphoinositide 3-kinase (PI3K) is fully responsible for AKT activation (26,27). AKT T308 is phosphorylated by phosphoinositide-dependent kinase 1 (PDK1), which is achieved by phosphatidylinositol (3,4,5)-trisphosphate-mediated membrane recruitment of PDK1. The activation of mammalian target of rapamycin complex 2 (mTORC2), which is the main kinase responsible for phosphorylation of AKT S473, also requires PI3K activity. Accordingly, PI3K inhibitors such as LY294002 block not only AKT phosphorylation, but also AKT-mediated cellular functions such as glucose uptake (28).

To investigate the PI3K-dependency of IR-A48 induced events, we measured glucose uptake and AKT phosphorylation in 3T3-L1 adipocytes after pre-incubation with a PI3K inhibitor (LY294002) for 1 h. Not only glucose uptake induced by IR-A48 (200 nmol/l) was significantly blocked by LY294002, regardless of stimulation time (30 min and 2 h), but AKT phosphorylation by IR-A48 was also inhibited (Figure 6C and D). Therefore, as with insulin, AKT

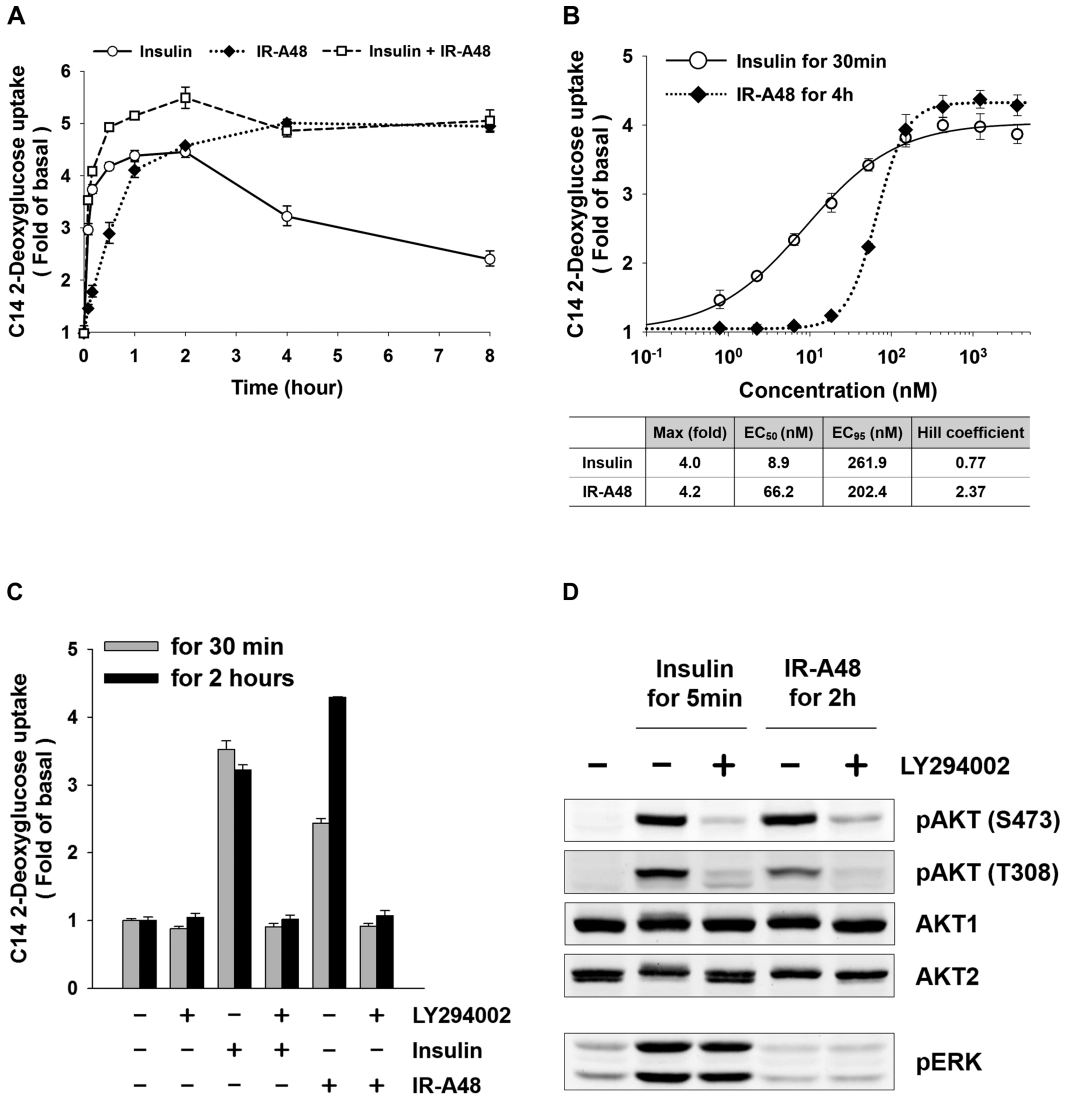

	Max (fold)	EC_{50} (nM)	EC_{95} (nM)	Hill coefficient
Insulin	4.0	8.9	261.9	0.77
IR-A48	4.2	66.2	202.4	2.37

Figure 6. IR-A48 stimulates glucose uptake through the PI3K pathway in 3T3-L1 adipocytes. (**A**) 2-Deoxy-D-glucose uptake was measured following incubation of adipocytes with 50 nmol/l insulin or 200 nmol/l IR-A48 for 5 min, 10 min, 30 min, 1 h, 2 h, 4 h and 8 h. (**B**) Cells were treated with increasing doses of insulin and IR-A48 for 30 min (insulin) or 4 h (IR-A48). To determine the EC_{50}, EC_{95} and Hill coefficient, data were fitted to a four-parameter logistic equation. (**C**) Before insulin or IR-A48 stimulation, cells were pre-incubated with 20 μmol/l LY294002 for 1 h. 2-deoxy-D-glucose uptake was measured after 30 min (gray bar) and 2 h (black bar). The data for glucose uptake are presented as the mean ± S.E. of three biological replicates and similar results were obtained from three independent experiments. (**D**) AKT phosphorylation was measured by western blotting to assess the effect of PI3K inhibition on IR-A48-induced phosphorylation.

phosphorylation and glucose uptake stimulated by IR-A48 in 3T3-L1 adipocytes are dependent on PI3K activity.

IR-A48 lowers blood glucose in mice

To confirm our results *in vivo*, we evaluated the effect of IR-A48 on blood glucose levels in mice. To prevent rapid degradation of the aptamer by 3′ exonucleases in the blood, inverted deoxy-thymidine (idT) was incorporated at the 3′-end of IR-A48. In mouse serum, idT conjugated IR-A48 was sufficiently stable to observe short-term *in vivo* glucose lowering ($t_{1/2}$ = 82 min) (Supplementary Figure S7). After fasting for 12 h, IR-A48 at doses of 10, 5 and 2.5 mg/kg were administered to mice through tail vein injection and blood glucose levels were measured for up to 120 min. At 30 min after injection, mice treated with 10 mg/kg IR-A48 exhibited significantly lowered blood glucose levels (59% of initial level), comparable to that achieved by administration of 0.6 unit/kg insulin (49% of initial level) (Figure 7). Notably, in contrast to insulin-treated mice, whose blood glucose levels recovered after 30 min, mice treated with IR-A48 exhibited continuously decreased blood glucose levels (53% of initial level) for 1 h, and the recovery of blood glucose levels occurred much more slowly than following insulin treatment, reflecting the *in vitro* data (Figure 6A). In addition, consistent with cell experiments, a scrambled aptamer (IR-A48 RC) also did not decrease blood glucose level in mice (Supplementary Figure S8). Thus, this result clearly shows that IR-A48 is effective both *in vivo* and *in vitro*, and demon-

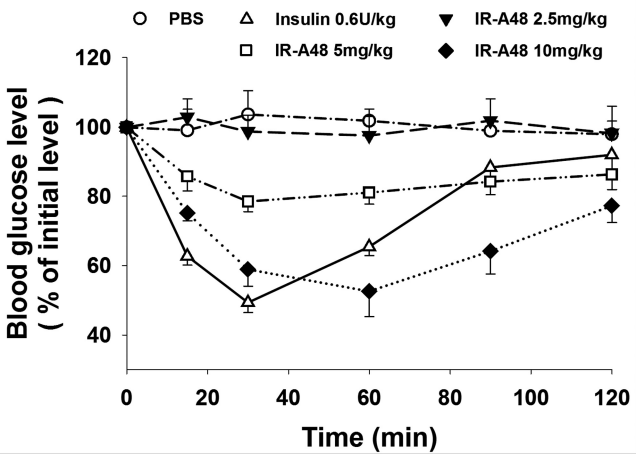

Figure 7. IR-A48 lowers blood glucose levels in mice to the same degree as insulin. Insulin (0.6 unit/kg), IR-A48 (2.5, 5 and 10 mg/kg) and PBS were administered to 12 h fasted C57Bl/6J mice by tail vein injection and blood glucose levels were measured at 15, 30, 60, 90 and 120 min after injection. The data were normalized to glucose levels determined just before injection. Values are given as the means ±S.E. ($n = 5$ mice/group).

strates that the allosteric modulation of IR by IR-A48 can control blood glucose levels independent of insulin.

DISCUSSION

In this study, we identified an agonistic IR aptamer, IR-A48, which is highly specific for IR without cross-activity for IGF-1R. IR-A48 binds to an allosteric site distinct from the orthosteric site for insulin binding and preferentially stimulates Y1150 phosphorylation in the IR kinase domain. Moreover, we demonstrated that the allosteric binding of IR-A48 not only stimulates activation of the IRS-AKT S473 pathway and glucose uptake in 3T3-L1 adipocytes, but also successfully lowers blood glucose levels in mice in a manner similar to insulin. However, unlike stimulation with insulin, activation of the MAPK pathway and the proliferation of MCF-7 cancer cells were not induced by IR-A48. Taken together, these results demonstrate that IR-A48 is a biased agonist of IR that selectively stimulates the metabolic activity of the receptor (glucose uptake) without mitogenic action (proliferation).

This is the first study to show that aptamer–protein interactions can not only differentially modulate receptor autophosphorylation (IR Y1150), but also induce specific signaling pathways and functional selectivity. To modulate receptor functions involved in the immune response, some dimeric or multivalent ligands using non-functional aptamers were developed. However, their activity is based on receptor oligomerization mediated by aptamer bridges, rather than by a change in receptor conformation induced by aptamer–receptor interactions (29–31). Until now, aptamer-mediated receptor activation has been reported only for an aptamer that binds tropomyosin receptor kinase B (TrkB). However, this aptamer not only acts as a simple partial agonist that is not functionally different from an endogenous ligand, Brain Derived Neurotrophic Factor(BDNF), but also partially inhibits BDNF-mediated TrkB activation (32). The concept of a biased agonist able to selectively modulate receptor functions has been well-established and several studies described small chemicals, peptides and antibodies that act as biased agonists (33,34). Our results indicate that it is possible to develop allosteric-biased agonists to a specific membrane receptor through SELEX.

A key aspect of biased agonists is their capacity to provide a therapeutic advantage for treating diseases by avoiding on-target adverse effects that arise from the activation of undesirable signaling pathways (33,34). In this respect, biased IR modulation is considered a valuable modality for diabetes care. Diabetes mellitus patients suffer from deficient secretion of insulin resulting from pancreatic beta-cell death (Type 1 diabetes), or insulin resistance, in which peripheral tissues fail to respond to insulin stimulation (Type 2 diabetes). To date, a variety of insulin analogs that have modified amino acid sequences have been successfully used in diabetes patients for normal glycemic control. However, insulin treatment is also considered to promote cell proliferation and the amino acid modifications of some insulin analogs increase their binding affinity and activation of IGF1-R (23,35,36). Accordingly, long-term use of insulin analogs for diabetes care has raised concerns regarding increased cancer risk (37) and several epidemiological reports showed correlations between prolonged insulin treatment and increased cancer risk (38–42). Therefore, the development of a biased IR agonist that selectively induces glucose uptake without a mitogenic effect would present a viable alternative to insulin therapy (43). IR-A48 raises the possibility of the use of a biased IR agonist to control blood glucose without the potential increase in cancer risk. In particular, the high specificity of IR-A48 for IR (and not IGF-1R) and its ability to bind allosterically without interfering with insulin binding are notable advantages as a therapeutic agent for diabetes care. We believe that IR-A48 represents a novel strategy for allosterically facilitating insulin action and improving glycemic control in diabetes patients.

The biased nature of IR-A48-mediated IR modulation likely results from the altered structural state induced by the allosteric binding of IR-A48. Evidence for this comes from the pattern of IR autophosphorylation induced by IR-A48 binding compared to insulin. In our study, we demonstrated that IR-A48 preferentially stimulates Y1150 phosphorylation in the IR kinase domain. Interestingly, the current activation model for IR autophosphorylation cannot sufficiently explain how Y1150-biased phosphorylation occurs in the absence of Y1146 and 1151 phosphorylation. Currently, phosphorylation of Y1146, Y1150 and Y1151 in the IR kinase domain is believed to occur via *trans*-autophosphorylation (44,45). Y1146, Y1150 and Y1151 are located in the activation loop (A-loop) in the IR kinase domain (46). According to the current model, insulin binding induces a conformational change that causes the IR kinase domains to approach each other, which activates the IR kinase by phosphorylating the opposite three tyrosine residues in the A-loop. Moreover, biochemical data demonstrate that artificial dimerization or aggregation of the IR kinase domain mainly leads to tri-phosphorylation of the A-loop (pY1146-pY1150-pY1151) (15). One plausible explanation for the observed IR-A48-mediated Y1150-biased phosphorylation is the presence of an independent mecha-

nism specific for Y1150 phosphorylation that is not related to *trans*-phosphorylation. However, this remains unknown due to the absence of structural evidence to clarify how the allosteric binding of IR-A48 differentially modulates IR conformation. Thus, a major question to be addressed in further studies will be the identification of the binding site of IR-A48 and the subsequent change in IR conformation.

The Y1150-biased phosphorylation induced by IR-A48 also differentially regulates signaling beyond simple receptor modulation. The data presented here reveal that IR-A48 can dramatically increase the phosphorylation of proteins in the IRS-AKT pathway such as IRS-1, AKT, AS160, FOXO1/3a and GSK3 in 3T3-L1 adipocytes. Conversely, phosphorylation of Src homology 2 domain containing transforming protein (SHC) and ERK in the MAPK pathway was not significantly stimulated by IR-A48. Previous studies on agonists that target the extracellular domain of IR reported similar biased signaling and functional selectivity. For instance, the synthetic peptide S597 and allosteric antibody XMetA induced higher activation of the IRS-AKT pathway than the MAPK pathway. Moreover, S597 induced the activation of glycogen synthesis in L6 myoblast cells and XMetA markedly improved glycemic control in diabetic model mice, but neither had an effect on cell proliferation (47,48). However, at present, the mechanism that mediates biased signaling and functional selectivity at the receptor level remains unknown. Our data imply that the IR Y1150-biased phosphorylation by IR-A48 is a unique property involved in functional selectivity. Although S597 and XMetA have signaling properties similar to IR-A48, IR Y1150-biased phosphorylation was not documented, because only total tyrosine phosphorylation was observed. Thus, mapping the IR tyrosine phosphorylation induced by other IR agonists will be necessary. If they share the same Y1150-biased activity, this would be clear evidence that IR Y1150 phosphorylation is a determinant of functional selectivity. In addition, the extracellular motif or structure of IR that regulates metabolism-specific signaling could be identified by comparing binding sites and analyzing the conformational changes induced by these agonists.

We also observed that AKT phosphorylation by IR-A48 is biased toward S473 rather than T308. The finding that IR-A48 sufficiently stimulated glucose uptake in 3T3-L1 adipocytes suggests that AKT T308 phosphorylation is not critically involved in glucose uptake. The specific roles of T308 and S473 in AKT activation are still unclear, but AKT kinase is fully activated when both residues are phosphorylated (49). Although the critical role of AKT in insulin-induced glucose uptake was verified using dominant-negative and constitutively-active mutants, the specific roles of S473 and T308 in this process have not been sufficiently studied (50–52). However, some studies showed that T308 and S473 have different effects on the phosphorylation of AKT substrates and AKT-mediated functions. For instance, disruption of mTORC2, which phosphorylates AKT S473, impairs FOXO1/3a phosphorylation, but has no effect on GSK3 and TSC2 phosphorylation (53,54). In addition, functionally, only AKT T308 phosphorylation, not S473, is correlated with survival of acute myeloid leukemia patients and AKT kinase activity in human non-small cell lung cancer (55,56). Thus, in 3T3-L1 adipocytes, AKT substrates that are involved in glucose uptake may be mainly regulated by AKT S473 rather than T308. Consistent with this, fat cell-specific ablation of Rictor, a subunit of mTORC2, in mice significantly impaired insulin-induced glucose uptake even though AKT T308 phosphorylation was maintained (57). Unfortunately, how IR Y1150-biased phosphorylation leads to AKT S473-biased phosphorylation remains an open question to be solved through further research.

Our understanding of the biased IR modulation by IR-A48 is incomplete, with a range of questions remaining to be answered. However, the concept of allosteric aptamers able to selectively modulate receptor functions suggests a novel strategy for research on receptor modulation and the development of more effective therapeutics. Advances in DNA synthetic methods and automation of the SELEX process make it possible to generate multiple target-specific aptamer libraries within weeks. In contrast to conventional screening using large numbers of non-specific compounds, aptamer technology has a crucial advantage in that it is able to generate candidate molecules with outstanding affinity and specificity to targeted receptors. Our study provides new direction for aptamer application: the development of allosteric receptor agonists able to modulate specific functions of the target receptors.

SUPPLEMENTARY DATA

Supplementary Data are available at NAR Online.

FUNDING

National Research Foundation of Korea (NRF) grant funded by the Korea government (MEST) [NRF-2015R1A2A1A13001834]. Funding for open access charge: NRF.
Conflict of interest statement. None declared.

REFERENCES

1. Tuerk,C. and Gold,L. (1990) Systematic evolution of ligands by exponential enrichment: RNA ligands to bacteriophage T4 DNA polymerase. *Science*, **249**, 505–510.
2. Ellington,A.D. and Szostak,J.W. (1990) In vitro selection of RNA molecules that bind specific ligands. *Nature*, **346**, 818–822.
3. Bates,P.J., Laber,D.A., Miller,D.M., Thomas,S.D. and Trent,J.O. (2009) Discovery and development of the G-rich oligonucleotide AS1411 as a novel treatment for cancer. *Exp. Mol. Pathol.*, **86**, 151–164.
4. Ng,E.W., Shima,D.T., Calias,P., Cunningham,E.T. Jr, Guyer,D.R. and Adamis,A.P. (2006) Pegaptanib, a targeted anti-VEGF aptamer for ocular vascular disease. *Nat. Rev. Drug Discov.*, **5**, 123–132.
5. Sundaram,P., Kurniawan,H., Byrne,M.E. and Wower,J. (2013) Therapeutic RNA aptamers in clinical trials. *Eur. J. Pharm. Sci.*, **48**, 259–271.
6. Luo,D. and Saltzman,W.M. (2000) Synthetic DNA delivery systems. *Nat. Biotechnol.*, **18**, 33–37.
7. Hopkins,A.L. and Groom,C.R. (2002) The druggable genome. *Nat. Rev. Drug Discov.*, **1**, 727–730.
8. Yildirim,M.A., Goh,K.I., Cusick,M.E., Barabasi,A.L. and Vidal,M. (2007) Drug-target network. *Nat. Biotechnol.*, **25**, 1119–1126.
9. Youngren,J.F. (2007) Regulation of insulin receptor function. *Cell. Mol. Life Sci.*, **64**, 873–891.
10. Leto,D. and Saltiel,A.R. (2012) Regulation of glucose transport by insulin: traffic control of GLUT4. *Nat. Rev. Mol. Cell Biol.*, **13**, 383–396.

11. American Diabetes Association. (2010) Diagnosis and classification of diabetes mellitus. *Diabetes Care*, **33**, S62–S69.
12. Lee,Y.J., Kim,I.S., Park,S.A., Kim,Y., Lee,J.E., Noh,D.Y., Kim,K.T., Ryu,S.H. and Suh,P.G. (2013) Periostin-binding DNA aptamer inhibits breast cancer growth and metastasis. *Mol. Ther.*, **21**, 1004–1013.
13. Lollo,B., Steele,F. and Gold,L. (2014) Beyond antibodies: new affinity reagents to unlock the proteome. *Proteomics*, **14**, 638–644.
14. Lawrence,M.C., McKern,N.M. and Ward,C.W. (2007) Insulin receptor structure and its implications for the IGF-1 receptor. *Curr. Opin. Struct. Biol.*, **17**, 699–705.
15. Baer,K., Al-Hasani,H., Parvaresch,S., Corona,T., Rufer,A., Nolle,V., Bergschneider,E. and Klein,H.W. (2001) Dimerization-induced activation of soluble insulin/IGF-1 receptor kinases: an alternative mechanism of activation. *Biochemistry*, **40**, 14268–14278.
16. Wilden,P.A., Kahn,C.R., Siddle,K. and White,M.F. (1992) Insulin receptor kinase domain autophosphorylation regulates receptor enzymatic function. *J. Biol. Chem.*, **267**, 16660–16668.
17. Gustafson,T.A., He,W., Craparo,A., Schaub,C.D. and O'Neill,T.J. (1995) Phosphotyrosine-dependent interaction of SHC and insulin receptor substrate 1 with the NPEY motif of the insulin receptor via a novel non-SH2 domain. *Mol. Cell. Biol.*, **15**, 2500–2508.
18. He,W., Craparo,A., Zhu,Y., O'Neill,T.J., Wang,L.M., Pierce,J.H. and Gustafson,T.A. (1996) Interaction of insulin receptor substrate-2 (IRS-2) with the insulin and insulin-like growth factor I receptors. Evidence for two distinct phosphotyrosine-dependent interaction domains within IRS-2. *J. Biol. Chem.*, **271**, 11641–11645.
19. Tartare-Deckert,S., Murdaca,J., Sawka-Verhelle,D., Holt,K.H., Pessin,J.E. and Van Obberghen,E. (1996) Interaction of the molecular weight 85K regulatory subunit of the phosphatidylinositol 3-kinase with the insulin receptor and the insulin-like growth factor-1 (IGF- I) receptor: comparative study using the yeast two-hybrid system. *Endocrinology*, **137**, 1019–1024.
20. Van Horn,D.J., Myers,M.G. Jr and Backer,J.M. (1994) Direct activation of the phosphatidylinositol 3′-kinase by the insulin receptor. *J. Biol. Chem.*, **269**, 29–32.
21. Kerkhoff,E. and Rapp,U.R. (1998) Cell cycle targets of Ras/Raf signalling. *Oncogene*, **17**, 1457–1462.
22. Pages,G., Lenormand,P., L'Allemain,G., Chambard,J.C., Meloche,S. and Pouyssegur,J. (1993) Mitogen-activated protein kinases p42mapk and p44mapk are required for fibroblast proliferation. *Proc. Natl. Acad. Sci. U.S.A.*, **90**, 8319–8323.
23. Lundby,A., Bolvig,P., Hegelund,A.C., Hansen,B.F., Worm,J., Lutzen,A., Billestrup,N., Bonnesen,C. and Oleksiewicz,M.B. (2015) Surface-expressed insulin receptors as well as IGF-I receptors both contribute to the mitogenic effects of human insulin and its analogues. *J. Appl. Toxicol.*, **35**, 842–850.
24. Shukla,A., Grisouard,J., Ehemann,V., Hermani,A., Enzmann,H. and Mayer,D. (2009) Analysis of signaling pathways related to cell proliferation stimulated by insulin analogs in human mammary epithelial cell lines. *Endocr. Relat. Cancer*, **16**, 429–441.
25. Taniguchi,C.M., Emanuelli,B. and Kahn,C.R. (2006) Critical nodes in signalling pathways: insights into insulin action. *Nat. Rev. Mol. Cell Biol.*, **7**, 85–96.
26. Franke,T.F., Yang,S.I., Chan,T.O., Datta,K., Kazlauskas,A., Morrison,D.K., Kaplan,D.R. and Tsichlis,P.N. (1995) The protein kinase encoded by the Akt proto-oncogene is a target of the PDGF-activated phosphatidylinositol 3-kinase. *Cell*, **81**, 727–736.
27. Burgering,B.M. and Coffer,P.J. (1995) Protein kinase B (c-Akt) in phosphatidylinositol-3-OH kinase signal transduction. *Nature*, **376**, 599–602.
28. Sanchez-Margalet,V., Goldfine,I.D., Vlahos,C.J. and Sung,C.K. (1994) Role of phosphatidylinositol-3-kinase in insulin receptor signaling: studies with inhibitor, LY294002. *Biochem. Biophys. Res. Commun.*, **204**, 446–452.
29. Pratico,E.D., Sullenger,B.A. and Nair,S.K. (2013) Identification and characterization of an agonistic aptamer against the T cell costimulatory receptor, OX40. *Nucleic Acid Ther.*, **23**, 35–43.
30. McNamara,J.O., Kolonias,D., Pastor,F., Mittler,R.S., Chen,L., Giangrande,P.H., Sullenger,B. and Gilboa,E. (2008) Multivalent 4–1BB binding aptamers costimulate CD8+ T cells and inhibit tumor growth in mice. *J. Clin. Invest.*, **118**, 376–386.
31. Dollins,C.M., Nair,S., Boczkowski,D., Lee,J., Layzer,J.M., Gilboa,E. and Sullenger,B.A. (2008) Assembling OX40 aptamers on a molecular scaffold to create a receptor-activating aptamer. *Chem. Biol.*, **15**, 675–682.
32. Huang,Y.Z., Hernandez,F.J., Gu,B., Stockdale,K.R., Nanapaneni,K., Scheetz,T.E., Behlke,M.A., Peek,A.S., Bair,T., Giangrande,P.H. *et al.* (2012) RNA aptamer-based functional ligands of the neurotrophin receptor, TrkB. *Mol. Pharmacol.*, **82**, 623–635.
33. Kenakin,T. (2011) Functional selectivity and biased receptor signaling. *J. Pharmacol. Exp. Ther.*, **336**, 296–302.
34. Violin,J.D., Crombie,A.L., Soergel,D.G. and Lark,M.W. (2014) Biased ligands at G-protein-coupled receptors: promise and progress. *Trends Pharmacol. Sci.*, **35**, 308–316.
35. Tennagels,N. and Werner,U. (2013) The metabolic and mitogenic properties of basal insulin analogues. *Arch. Physiol. Biochem.*, **119**, 1–14.
36. Ish-Shalom,D., Christoffersen,C.T., Vorwerk,P., Sacerdoti-Sierra,N., Shymko,R.M., Naor,D. and De Meyts,P. (1997) Mitogenic properties of insulin and insulin analogues mediated by the insulin receptor. *Diabetologia*, **40**(Suppl. 2), S25–S31.
37. Mannucci,E. (2012) Insulin therapy and cancer in type 2 diabetes. *ISRN Endocrinol.*, **2012**, 240634.
38. Li,D., Yeung,S.C., Hassan,M.M., Konopleva,M. and Abbruzzese,J.L. (2009) Antidiabetic therapies affect risk of pancreatic cancer. *Gastroenterology*, **137**, 482–488.
39. Hemkens,L.G., Grouven,U., Bender,R., Gunster,C., Gutschmidt,S., Selke,G.W. and Sawicki,P.T. (2009) Risk of malignancies in patients with diabetes treated with human insulin or insulin analogues: a cohort study. *Diabetologia*, **52**, 1732–1744.
40. Bowker,S.L., Majumdar,S.R., Veugelers,P. and Johnson,J.A. (2006) Increased cancer-related mortality for patients with type 2 diabetes who use sulfonylureas or insulin. *Diabetes Care*, **29**, 254–258.
41. Yang,Y.X., Hennessy,S. and Lewis,J.D. (2004) Insulin therapy and colorectal cancer risk among type 2 diabetes mellitus patients. *Gastroenterology*, **127**, 1044–1050.
42. Janghorbani,M., Dehghani,M. and Salehi-Marzijarani,M. (2012) Systematic review and meta-analysis of insulin therapy and risk of cancer. *Horm. Cancer*, **3**, 137–146.
43. Vigneri,R., Squatrito,S. and Frittitta,L. (2012) Selective insulin receptor modulators (SIRM): a new class of antidiabetes drugs? *Diabetes*, **61**, 984–985.
44. Ottensmeyer,F.P., Beniac,D.R., Luo,R.Z. and Yip,C.C. (2000) Mechanism of transmembrane signaling: insulin binding and the insulin receptor. *Biochemistry*, **39**, 12103–12112.
45. Hubbard,S.R., Mohammadi,M. and Schlessinger,J. (1998) Autoregulatory mechanisms in protein-tyrosine kinases. *J. Biol. Chem.*, **273**, 11987–11990.
46. Hubbard,S.R., Wei,L., Ellis,L. and Hendrickson,W.A. (1994) Crystal structure of the tyrosine kinase domain of the human insulin receptor. *Nature*, **372**, 746–754.
47. Bhaskar,V., Goldfine,I.D., Bedinger,D.H., Lau,A., Kuan,H.F., Gross,L.M., Handa,M., Maddux,B.A., Watson,S.R., Zhu,S. *et al.* (2012) A fully human, allosteric monoclonal antibody that activates the insulin receptor and improves glycemic control. *Diabetes*, **61**, 1263–1271.
48. Jensen,M., Hansen,B., De Meyts,P., Schaffer,L. and Urso,B. (2007) Activation of the insulin receptor by insulin and a synthetic peptide leads to divergent metabolic and mitogenic signaling and responses. *J. Biol. Chem.*, **282**, 35179–35186.
49. Alessi,D.R., Andjelkovic,M., Caudwell,B., Cron,P., Morrice,N., Cohen,P. and Hemmings,B.A. (1996) Mechanism of activation of protein kinase B by insulin and IGF-1. *EMBO J.*, **15**, 6541–6551.
50. Hajduch,E., Alessi,D.R., Hemmings,B.A. and Hundal,H.S. (1998) Constitutive activation of protein kinase B alpha by membrane targeting promotes glucose and system A amino acid transport, protein synthesis, and inactivation of glycogen synthase kinase 3 in L6 muscle cells. *Diabetes*, **47**, 1006–1013.
51. Cong,L.N., Chen,H., Li,Y., Zhou,L., McGibbon,M.A., Taylor,S.I. and Quon,M.J. (1997) Physiological role of Akt in insulin-stimulated translocation of GLUT4 in transfected rat adipose cells. *Mol. Endocrinol.*, **11**, 1881–1890.
52. Kohn,A.D., Summers,S.A., Birnbaum,M.J. and Roth,R.A. (1996) Expression of a constitutively active Akt Ser/Thr kinase in 3T3-L1 adipocytes stimulates glucose uptake and glucose transporter 4 translocation. *J. Biol. Chem.*, **271**, 31372–31378.

53. Guertin,D.A., Stevens,D.M., Thoreen,C.C., Burds,A.A., Kalaany,N.Y., Moffat,J., Brown,M., Fitzgerald,K.J. and Sabatini,D.M. (2006) Ablation in mice of the mTORC components raptor, rictor, or mLST8 reveals that mTORC2 is required for signaling to Akt-FOXO and PKCalpha, but not S6K1. *Dev. Cell*, **11**, 859–871.
54. Jacinto,E., Facchinetti,V., Liu,D., Soto,N., Wei,S., Jung,S.Y., Huang,Q., Qin,J. and Su,B. (2006) SIN1/MIP1 maintains rictor-mTOR complex integrity and regulates Akt phosphorylation and substrate specificity. *Cell*, **127**, 125–137.
55. Gallay,N., Dos Santos,C., Cuzin,L., Bousquet,M., Simmonet Gouy,V., Chaussade,C., Attal,M., Payrastre,B., Demur,C. and Recher,C. (2009) The level of AKT phosphorylation on threonine 308 but not on serine 473 is associated with high-risk cytogenetics and predicts poor overall survival in acute myeloid leukaemia. *Leukemia*, **23**, 1029–1038.
56. Vincent,E.E., Elder,D.J., Thomas,E.C., Phillips,L., Morgan,C., Pawade,J., Sohail,M., May,M.T., Hetzel,M.R. and Tavare,J.M. (2011) Akt phosphorylation on Thr308 but not on Ser473 correlates with Akt protein kinase activity in human non-small cell lung cancer. *Br. J. Cancer*, **104**, 1755–1761.
57. Kumar,A., Lawrence,J.C. Jr, Jung,D.Y., Ko,H.J., Keller,S.R., Kim,J.K., Magnuson,M.A. and Harris,T.E. (2010) Fat cell-specific ablation of rictor in mice impairs insulin-regulated fat cell and whole-body glucose and lipid metabolism. *Diabetes*, **59**, 1397–1406.